Supporting Information

Two polyoxovanadate-based metal-organic polyhedra with "near-miss Johnson solid" geometry

Yaru Gong,‡[a] Yanli Tao,‡[a] Na Xu,[a] Chunyi Sun,[a] Xinlong Wang*[a] and Zhongmin Su*[ab]

[a] *Key Laboratory of Polyoxometalate Science of Ministry of Education, Northeast Normal University, Changchun, Jilin, 130024 (China).*

[b] *Jilin Provincial Science and Technology Innovation Center of Optical Materials and Chemistry, School of Chemistry and Environmental Engineering, Changchun University of Science and Technology, Changchun, Jilin, 130022 (China).*

*Corresponding author. E-mail address: wangxl824@nenu.edu.cn; zmsu@nenu.edu.cn.

Contents

Figure S4. The experimental and simulated powder X-Ray diffraction patterns for $[NbV_5O_{11}(SO_4)_6]^{9-}$.

Figure S5. The experimental and simulated powder X-Ray diffraction patterns for **VMOP-27** and **VMOP-28**.

Figure S6. IR spectra of **VMOP-27** and **VMOP-28**.

Figure S7. TGA curves of **VMOP-27** and **VMOP-28**.

Figure S8. Temperature dependence of the inverse magnetic susceptibility χ_M^{-1} for **VMOP-27** and **VMOP-28** between 2 and 300 K.

1. Materials and Methods

All chemical reagents were purchased from commercial sources and used without further purification. PXRD patterns were recorded ranging from 5° to 50° at room temperature on a Siemens D5005 diffractometer with Cu Kα (λ = 1.5418 Å). Thermogravimetric analysis (TGA) of the samples was performed using a PerkinElmer TG-7 analyzer heated from 25 °C to 800 °C at the heating rate of 10 °C·min^{-1} under a dry nitrogen flow. Elemental analyses (CHN) were conducted on a PerkinElmer 2400 CHN Elemental analyzer. The FT-IR spectra were measured on an Alpha Centaurt FT/IR spectrophotometer in the range 4000−400 cm^{-1} using KBr pellets. Variable temperature magnetic susceptibility data were obtained in the temperature range of 2–300 K using a SQUID magnetometer (Quantum Design, MPMS-5) with an applied field of 1000 Oe.

2. Synthesisand Characterization

(1) Synthesis of **VMOP-27**:

$VOSO_4 \cdot xH_2O$ (0.03 g), $NbCl_5$ (0.01 g) and 1,3,5-Benzenetricarboxylic acid (0.025 g) in 2 ml DMF (*N,N*-Dimethylformamide), 0.3 ml CH_3OH (methanol) and 0.2mL CH_3CN (acetonitrile) were placed in a Parr Teflon-lined stainless steel vessel heated to 130 °C and held at this temperature for 2 days. After slow cooling to room temperature, green crystals were obtained (washed with CH_3OH) with a yield of 30% based on H_3BTC. Elemental analysis (%) cacld: C, 24.10; H, 3.32; N, 5.02. Found: C, 23.79; H, 2.87; N, 4.35. IR (KBr, cm^{-1}): 3444 (br), 3032 (w), 2778 (w), 1617 (s), 1566(s), 1447 (s), 1390 (vs), 1110 (m), 1009 (m), 980 (s), 759 (s), 720 (s), 635 (s), 502 (m).

(2) Synthesis of **VMOP-28**:

$VOSO_4 \cdot xH_2O$ (0.02 g), Na_2WO_4 (0.01 g) and 1,3,5-Benzenetricarboxylic acid (0.02 g) in 2 ml DMF (*N,N*-Dimethylformamide), 0.5 ml CH_3OH (methanol) and a drop of hydrochloric acid were placed in a Parr Teflon-lined stainless steel vessel heated to 130 °C and held at this temperature for 2 days. After slow cooling to room temperature, green crystals were obtained (washed with CH_3OH) with a yield of 50% based on H_3BTC. Elemental analysis (%) cacld: C, 22.41; H, 2.75; N, 4.02. Found: C, 21.58; H, 2.94; N, 4.31. IR (KBr, cm^{-1}): 3027(m), 2779(m), 2457(w), 1657(m), 1612(s), 1561(s), 1445(s), 1386(s), 1105(m), 975(m), 800(w), 754(m), 716(m), 632(m), 578(m), 490(m).

Supplement: In the synthesis of **VMOP-27** and **VMOP-28**, we had tried some different vanadium source, such as $NaVO_3$, Na_3VO_4, NH_4VO_3, VCl_3 and V_2O_5, but they are not good for the synthesis metal-organic polyhedra.

Table S1. Crystallographic data for **VMOP-27**.

Empirical formula	$C_{168}H_{276}Cl_4N_{30}Nb_4O_{180}S_7V_{40}$
Formula weight	8371.63
Crystal system	Tetragonal
Space group	*I-42m*
Temperature	273 (2) K
Wavelength	0.71073 Å
Unit-cell dimensions	a = b =21.854 (3) Å, c = 44.273 (6) Å α = β =γ = 90°
Volume	21145 (6) $Å^3$
Z	2
Density (calculated)	1.315 g/cm^3
Absorption coefficient	1.077 mm^{-1}
F(000)	8396
Limiting indices	-26<=h<=26, -25<=k<=26, -51<=l<=52
Theta range for data collection	2.948 to 25.109 °
Reflections collected	54581
Independent reflections	7098 [R(int) = 0.0957]
Completeness to theta = 25.00°	99 %
Refinement method	Full-matrix least-squares on F^2
Data / restraints / parameters	9693 / 1094 / 487

Goodness-of-fit on F^2	1.009
Final R indices [I > 2sigma(I)]	R1 = 0.0647, wR2 = 0.1754
R indices (all data)	R1 = 0.0957, wR2 = 0.1979
Largest diff. peak and hole	0.761 and -1.994 eA^{-3}

[a]$R_1 = \Sigma||F_o|-|F_c||/\Sigma|F_o|$; [b]$wR_2=\{\Sigma\,[w(F_o^2-F_c^2)^2]/\Sigma\,[w(F_o^2)^2]\}^{1/2}$

Table S2. Crystallographic data for **VMOP-28.**

Empirical formula	$C_{156}H_{228}Cl_4N_{24}O_{176}S_6V_{40}W_4$
Formula weight	8362.77
Crystal system	Monoclinic
Space group	*C2/c*
Temperature	296 (2) K
Wavelength	0.71073 Å
Unit-cell dimensions	a = 41.892 (5) Å, b = 21.947 (2) Å, c =46.700 (5) Å α =γ = 90 °, β = 103.267 (4) °
Volume	41791 (8) $Å^3$
Z	4
Density (calculated)	1.329 g/cm^3
Absorption coefficient	2.072 mm^{-1}
F(000)	16480
Limiting indices	-48<=h<=49, -25<=k<=26, -55<=l<=55
Theta range for data collection	2.176-25.136°
Reflections collected	105495
Independent reflections	26809 [R(int) = 0.0551]
Completeness to theta = 25.00°	98.5 %
Refinement method	Full-matrix least-squares on F^2
Data / restraints / parameters	36825 / 1638/ 1761
Goodness-of-fit on F^2	1.018
Final R indices [I > 2sigma(I)]	R1 = 0.0612, wR2 = 0.1640
R indices (all data)	R1 = 0.0883, wR2 = 0.1853
Largest diff. peak and hole	2.571 and -3.366 eA^{-3}

[a]$R_1 = \Sigma||F_o|-|F_c||/\Sigma|F_o|$; [b]$wR_2=\{\Sigma\,[w(F_o^2-F_c^2)^2]/\Sigma\,[w(F_o^2)^2]\}^{1/2}$

Table S3. BVS results for the vanadium and niobium atoms in $[NbV_5O_6(\mu_3\text{-}O)_5(SO_4)(COO)_5]^{4-}$.

Atom	BVS calc. for V
V1	3.910
V2	4.033
V3	3.804
V4	3.937

V5	4.122
Atom	BVS calc. for Nb
Nb	5.119

Table S4. BVS results for the vanadium and tungsten atoms in $[WV_5O_6(\mu_3\text{-}O)_5(SO_4)(COO)_5]^{3-}$.

Atom	BVS calc. for V
V1	4.267
V2	4.243
V3	4.087
V4	4.117
V5	4.091
Atom	BVS calc. for W
W	6.060

Table S5. The structural analysis of **SP-38**.

Name	Kinds of SBUs	Vertices
SP-38	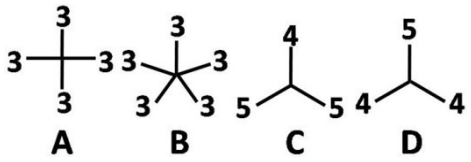	4

Table S6. The geometric parameters of simplified polyhedra which are including faces (F), edges (E), vertices (V), rotation groups and the dihedral angles between different faces. A triangle, a quadrangle, a pentagon are abbreviated as {3}, {4} and {5}.

Name	Faces	Edges	Edge and dihedral angles	Vertices	Group
SP-38	*2*•6 {3} 2+*4*•3+4+4 {4} 4 {5}	*12*•3 <3•4> *4*•4 <4•4>	172°14′35″/172°45′04″/166°27′14″/167°3′54″/151°47′56″/154°28′30″/154°14′28″/150°35′20″/150°34′23″/143°4′34″/148°45′58″/149°54″/141°32″/149°28′37″/140°51′29″/137°44′38″/139°41′06″/137°23′28″ 141°5′10″/141°41′42″/133°20′46″/138°56′53″/139°49′23″/133°30′32″/129°1′	*4*•4 (3•4^3) 4+*8*•2 (3•4•5•4)	$[2, 4]^+$ D_2

			26″/129°28′12″		
		4•5 <4•5>	158°18′29″/156°34′48″/150°20′49″/156°35′53″/144°53′49″/148°54′07″/144°23′24″/130°31′19″/135°26′02″/132°56′46″/136°22′30″		

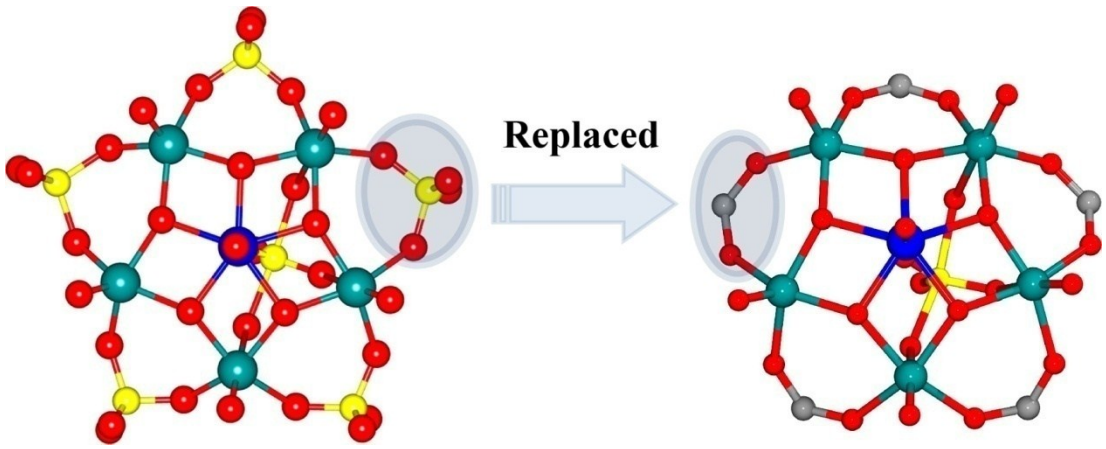

Figure S1. The ball-and-stick representation of the pentanuclear SBB [$MV_5O_6(\mu_3\text{-}O)_5(SO_4)_6$] and [$MV_5O_6(\mu_3\text{-}O)_5(SO_4)(COO)_5$].

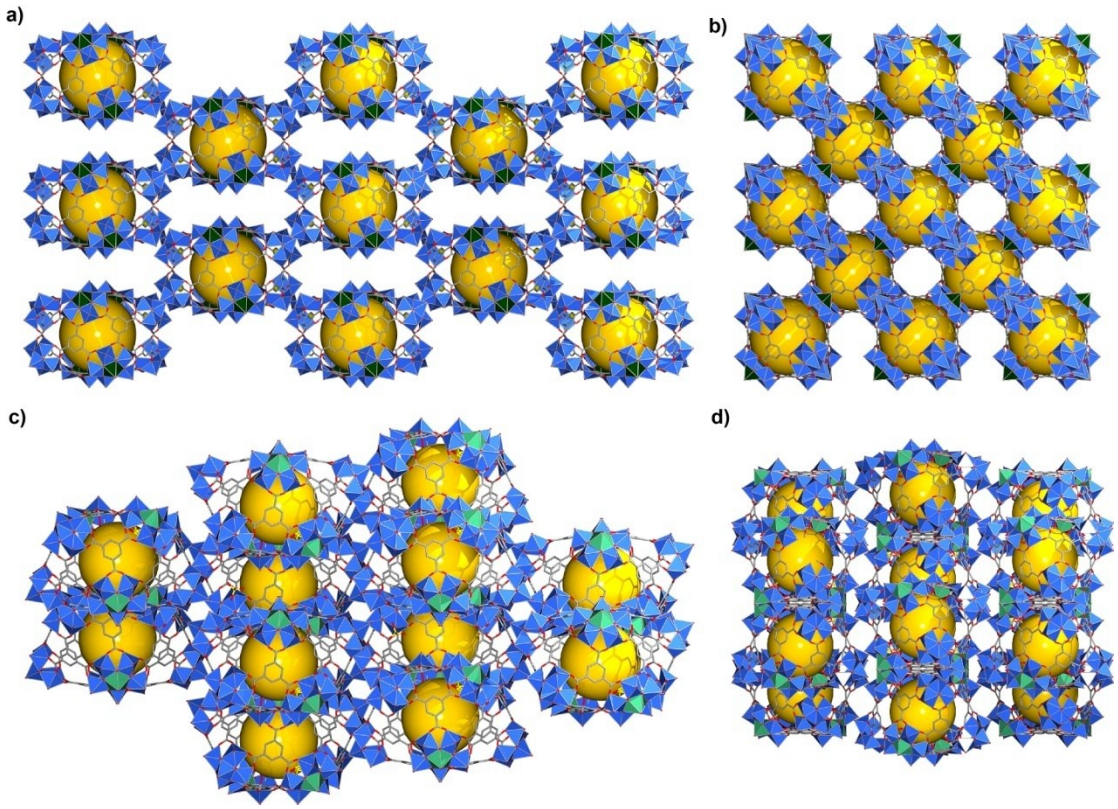

Figure S2. The packing representation of **VMOP-27** and **VMOP-28** with view in the direction of the crystallographic *a* axis (a, c) and *c* axis (b, d).

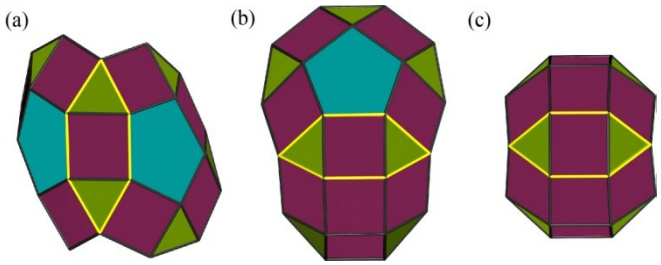

Figure S3. The connection mode between *J4* and *J5*: *J5* – *J5*, *J5* – *J4* and *J4* – *J4*.

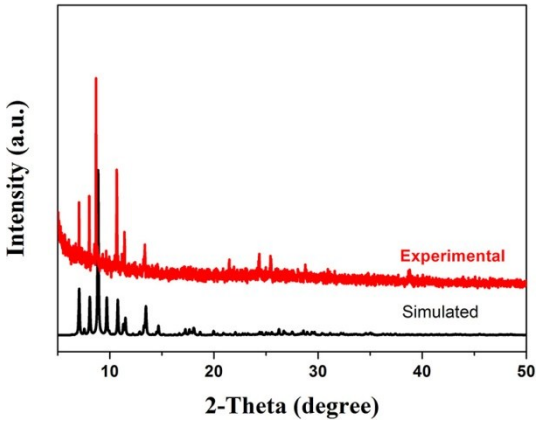

Figure S4. The experimental and simulated powder X-Ray diffraction patterns for $[NbV_5O_{11}(SO_4)_6]^{9-}$.

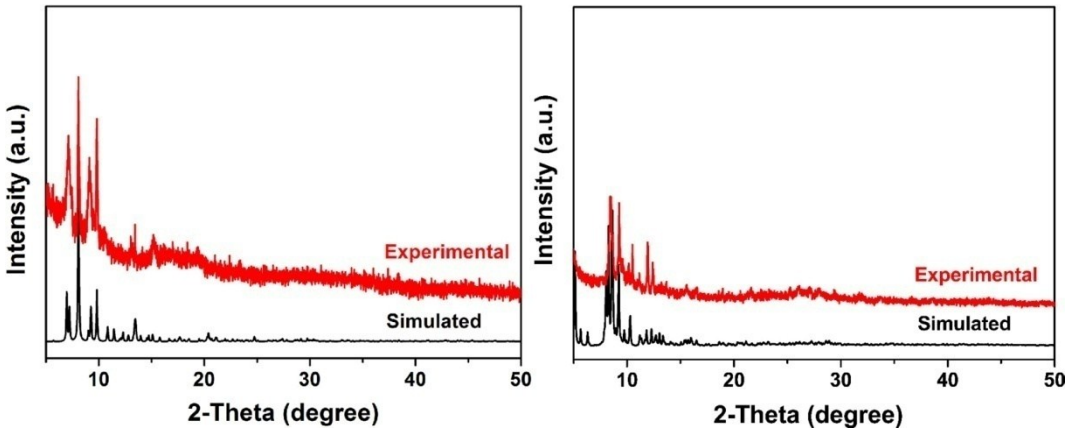

Figure S5. Experimental and simulated powder X-Ray diffraction patterns for **VMOP-27** and **VMOP-28**.

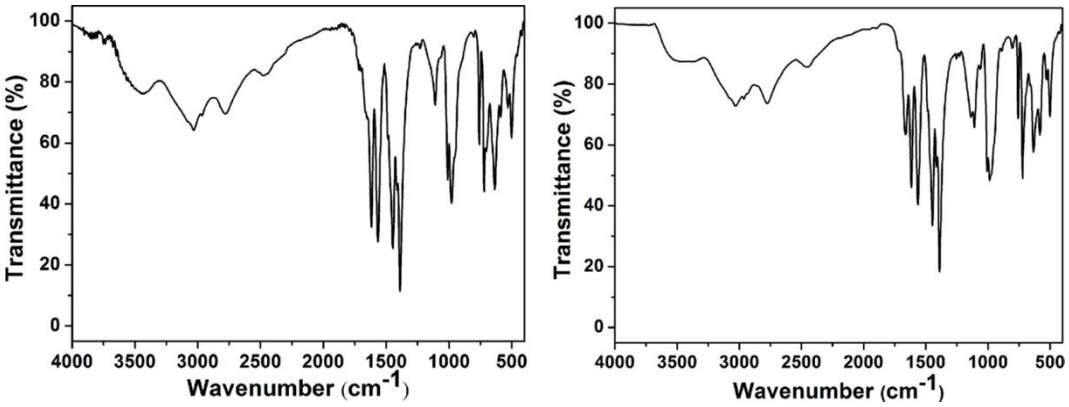

Figure S6. IR spectrum of **VMOP-27** and **VMOP-28.**

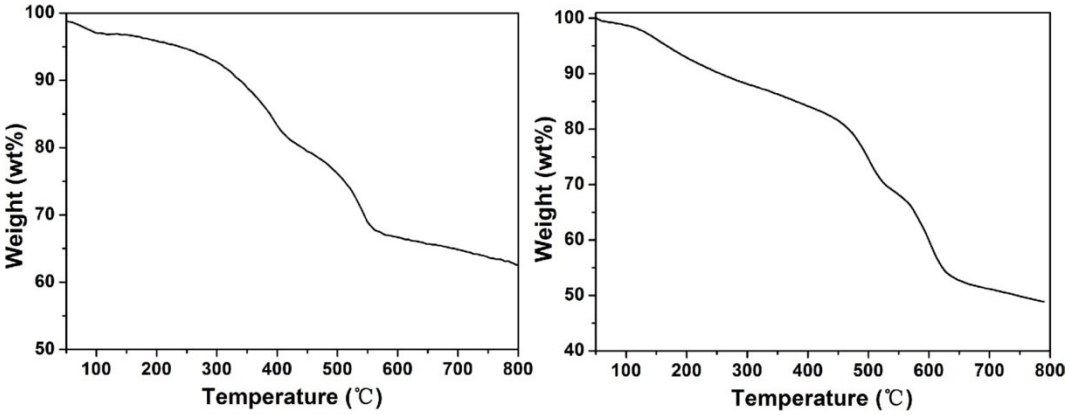

Figure S7. TGA curve of **VMOP-27** and **VMOP-28.**

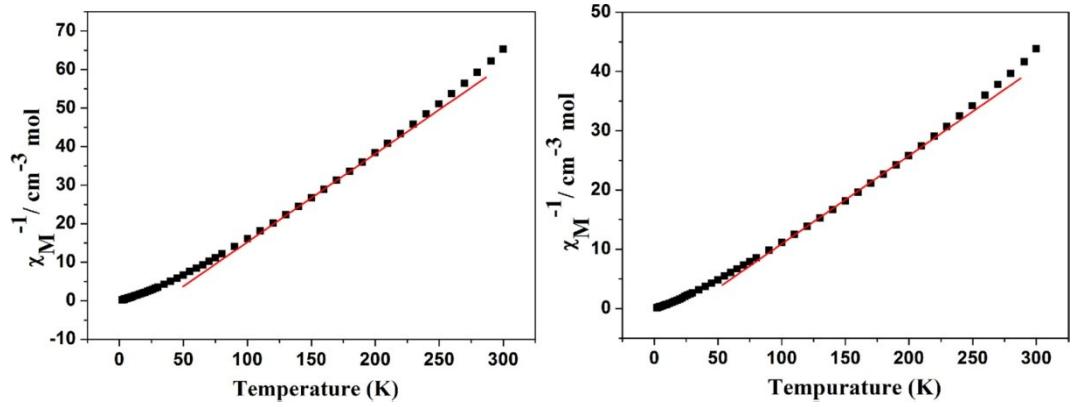

Figure S8. The temperature dependence of the inverse magnetic susceptibility χ_M^{-1} for **VMOP-27** between 2 and 300 K.